Europ. J. Protistol. 38, 247–265 (2002)

http://www.urbanfischer.de/journals/ejp

European Journal of
PROTISTOLOGY

New diplokaryotic microsporidia (Phylum Microsporidia) from freshwater bryozoans (Bryozoa, Phylactolaemata)

Elizabeth U. Canning[1,*] Dominik Refardt[2,6], Charles R. Vossbrinck[3], Beth Okamura[4] and Alan Curry[5]

[1]Department of Biological Sciences, Imperial College of Science, Technology and Medicine, London SW7 2AZ, UK; E-mail: e.canning@ic.ac.uk
[2]Zoologisches Institut, Universität Basel, Rheinsprung 9, CH-4051, Basel, Switzerland
[3]The Connecticut Agricultural Experiment Station, 123 Huntington Street, New Haven, Connecticut 06504, U.S.A.
[4]Department of Animal and Microbial Sciences, University of Reading, Whiteknights, Reading RG6 6AJ, U.K.
[5]Public Health Laboratory, Withington Hospital, Manchester M20 2LR

Received: 22 February 2002; 12 June 2002. Accepted: 13 June 2002

Three new species of microsporidia from freshwater bryozoans were investigated by microscopy and rDNA sequencing. These microsporidia and the previously described *Nosema cristatellae* have been ascribed to new genera, *Pseudonosema* gen. nov. for *N. cristatellae* from *Cristatella mucedo*, *Trichonosema* gen. nov. for *Trichonosema pectinatellae* sp. nov. from *Pectinatella magnifica* and *Bryonosema* gen. nov. for *Bryonosema plumatellae* sp. nov. from *Plumatella nitens* and for *Bryonosema tuftyi* sp. nov. from *Plumatella* sp. The new genera have been placed in a new family Pseudonosematidae with the following characters: diplokaryotic, disporoblastic and development in direct contact with host cell cytoplasm; spores of known species large with numerous polar tube coils; exospore dense with spiky extensions; or without spiky extensions and constructed of one or two layers; endospore and exospore thinned over the anchoring disc; anchoring disc ovoid with denser boundary around lucent interior penetrated by the inner core of the polar tube; polar sac small, umbrella-like; polar tube coils arranged as a single row anteriorly and posteriorly and as 2 or 3 rows in the middle; prominent reticulate Golgi system in sporoblasts and immature spores. Analysis of 16S rDNA by Baysian inference, maximum likelihood and parsimony placed all four species from bryozoans in one clade but the genera *Trichonosema* and *Pseudonosema* were separated from *Bryonosema* by the genera *Janacekia* and *Bacillidium*, which, on morphological grounds, cannot be included in the new family. The species are identified by morphological characters and their small subunit rDNA sequences.

Key words: Bryozoa; Microsporidia; Molecular phylogeny; *Bryonosema* gen. nov.; *Pseudonosema* gen. nov.; *Trichonosema* gen. nov.

*Address for correspondence: E. U. Canning, Imperial College at Silwood Park, Ascot, Berks SL5 7PY, UK; Fax: 020 7594 2339.

[6]Present address: Department de Biologie, Ecologie et Evolution, Université de Fribourg, Chemin du Musee 10, 1700 Fribourg, Switzerland.

0932-4739/02/38/03-247 $ 15.00/0

Introduction

The first mention of microsporidian infection of bryozoans is that of Thélohan (1895) who used the name *Glugea bryozoides* (Korotneff 1892) for the parasites seen by Korotneff (1892) in *Alcyonella fungosa* (now *Plumatella fungosa*) collected in Russia. Korotneff (1892) observed early stages of the parasite in the funiculus and later stages free in the body cavity. He named the species *Myxosporidium bryozoides* and attributed it to the "Myxosporidien". However his illustrations of spores like melon seeds (Melonensamen) suggested to Thélohan (1895) that they were microsporidia, rather than myxosporidia, and he proposed placing the species in the genus *Glugea*. The microsporidian interpretation was followed by Labbé (1899) but he transferred the species to the genus *Nosema*. If we accept the view that Korotneff's parasites were microsporidia, the generic name *Myxosporidium* would be confusing as a genus in the phylum Microsporidia and the species cannot be placed in a known microsporidian genus for lack of data. It may not be possible to identify it again, if microsporidia are found in *P. fungosa*. We propose to use the group name *Microsporidium* for this species, although it might be more appropriate to declare that the previously given names are *nomina nuda*.

A microsporidium infecting cells of the epithelium of *Cristatella mucedo* in England was described and named *Nosema cristatellae* by Canning et al. (1997). While collecting specimens of the bryozoans *Pectinatella magnifica* and *Plumatella nitens* in the U.S.A. and *Plumatella* sp. in England, specimens were found infected with microsporidia. Ultrastructural investigations revealed striking similarities in their development and spore structure and that all of them have characters in common with the genus *Nosema*: they develop in direct contact with host cell cytoplasm, have diplokaryotic nuclei and disporoblastic sporogony. However, phylogenetic analysis of sequences of 16S rDNA indicated that the new species are closely related to one another and to *Nosema cristatellae* but are distant from true *Nosema* species, of which the type species, *Nosema bombycis*, is a parasite of the silkworm (*Bombyx mori*), a lepidopteran. We propose to place the species from *P. magnifica* in a new genus as *Trichonosema pectinatellae* n.gen., n.sp. and the species from *P. nitens* and *Plumatella* sp. in another new genus *Bryonosema* n.gen. The species in *P. nitens* is named *Bryonosema plumatellae* n.sp. and the species in *Plumatella* sp. is named *Bryonosema tuftyi* n.sp. We also propose to transfer *N. cristatellae* to a new genus as *Pseudonosema cristatellae* (Canning, Okamura and Curry 1997).

Materials and methods

Microsporidia were encountered by chance in 1999 during an investigation of field prevalences of myxozoans in bryozoans. *Pectinatella magnifica* colonies were collected from the undersurface of leaves of American lotus, *Nelumbo lutea*, in Cowan Lake, Ohio, U.S.A. and from a submerged log in Big Evans Lake, Michigan, U.S.A. *Plumatella nitens* was collected from the stems of rushes, *Scirpus* sp., in Big Evans Lake. A single large (5.0 cm) colony of an unidentified *Plumatella* sp. growing on a submerged branch and two colonies of *Cristatella mucedo* on stems of water lilies *Nymphoides peltata* were collected from Tufty's Corner Lake, Berkshire, U.K. Except for one collection of *P. magnifica*, when 34 out of 72 (47%) small colonies on ten lotus leaves were found infected, no prevalence figures were obtained.

Zooids of all specimens were examined with a dissecting microscope at 12–50× magnification, when large cells were seen circulating in the coelom. Pieces of the infected colonies were teased apart to release the infected cells, which were then squashed and examined at higher magnification. On determination that the cells were infected with microsporidia not myxozoans, additional pieces of the colonies were fixed in glutararaldehyde for electron microscopy (em) or retained fresh or in ethanol for ribosomal DNA sequencing.

The microsporidia from *P. magnifica* collected from Cowan Lake and Big Evans Lake proved to be identical at the ultrastructural level and only the corresponding Cowan Lake sample of fresh spores was used to obtain the molecular data. For *P. nitens* pieces of a colony from Big Evans Lake (sample A) were fixed in glutaraldehyde for em and ethanol for sequencing. A sequence was also obtained from another colony of *P. nitens* (sample B), which had been retained as fresh spores but no corresponding ultrastructural study was carried out. Ultrastructural and molecular data (from an ethanol fixed sample) were obtained for the microsporidia in *Plumatella* sp. (Tufty's Corner Lake). Ultrastructural data and rDNA sequence data were also obtained for the microsporidia in *C. mucedo* but, in this case, the ultrastructural data were only used to confirm that the microsporidian species did not differ from *N. cristatellae.*

For electron microscopy, colony pieces were fixed in 2.5% glutaraldehyde in 0.1 M cacodylate buffer, post-fixed in 1% OsO_4, dehydrated in an ethanol series and embedded in Agar 100 resin (Agar Scientific, U.K.) via propylene oxide. Merogonic and sporogonic stages were generally well fixed but once the endospore layer had begun to form on the very large spores, preserva-

Table 1. Microsporidia, hosts and accession numbers of rDNA, together with data on *Basidiobolus ranarum* used as outgroup in the phylogenetic analysis.

Organism	Host	Accession number
Microsporidian sequences from GenBank		
Amblyospora californica	*Culex tarsalis*	U68473
Ameson michaelis	*Callinectes sapidus*	L15741
Antonospora scoticae	*Andrena scotica*	AF024655
Bacillidium sp.	*Lumbriculus* sp.	AF104087
Brachiola algerae	Anopheline mosquitoes	AF069063
Caudospora palustris	*Cnephia ornithophilia*	AF132544
Culicosporella lunata	*Culex pilosus*	AF027683
Cystosporogenes operophterae	*Operophtera brumata*	AJ302320
Edhazardia aedis	*Aedes aegypti*	AF027684
Encephalitozoon cuniculi	*Homo sapiens*	L17072
Encephalitozoon hellem	*Homo sapiens*	AF118142
Encephalitozoon intestinalis	*Homo sapiens*	L39113
Enterocytozoon bieneusi	*Homo sapiens*	AF024657
Endoreticulatus schubergi	*Lymantria dispar*	L39109
Flabelliforma magnivora	*Daphnia magna*	AJ302319
Glugea atherinae	*Atherina presbyter*	U15987
Glugoides intestinalis	*Daphnia magna, Daphnia pulex*	AF394525
Intrapredatorus barri	*Culex fuscanus*	AY013359
Janacekia debaisieuxi	*Simulium* sp.	AJ252950
Nosema apis	*Apis mellifera*	U97150
Nosema bombycis	*Bombyx mori*	L39111
Nosema granulosis	*Gammarus duebeni*	AJ011833
Nosema trichoplusiae	*Trichoplusia ni*	U09282
Nosema tyriae	*Tyria jacobaeae*	AJ012606
Nucleospora salmonis	Salmonid fish	U10883
Ordospora colligata	*Daphnia magna*	AF394529
Orthosomella operophterae	*Operophtera brumata*	AJ302317
Parathelohania anophelis	*Anopheles quadrimaculatus*	AF027682
Polydispyrenia simulii	*Simulium* sp.	AJ252960
Spraguea lophii	*Lophius americanus*	AF033197
Thelohania solenopsae	*Solenopsis invicta*	AF134205
Trachipleistophora hominis	*Homo sapiens*	AJ002605
Vairimorpha necatrix	*Malacosoma americanum*	Y00266
Vairimorpha imperfecta	*Plutella xylostella*	AJ131645
Vavraia oncoperae	*Weiseana* sp.	X74112
Visvesvaria acridophagus		AF024658
Vittaforma corneae	*Homo sapiens*	U11046
Other species from GenBank		
Basidiobolus ranarum (Fungi: Zygomycetes)		D29946
New sequences		
Bryonosema plumatellae	*Plumatella nitens*	
	Clone 1	AF484690
	Clone 2	AF484691
	Clone 3	AF484692
Bryonosema tuftyi	*Plumatella* sp.	AF484693
Pseudonosema cristatellae	*Cristatella mucedo*	AF484694
Trichonosema pectinatellae	*Pectinatella magnifica*	AF484695

tion of spore integrity was often below optimum. Sections were stained with uranyl acetate and lead citrate.

For extraction of DNA, samples were homogenised in a microfuge with a minipestle and processed with the DNeasy Tissue Kit (Qiagen, Basel, Switzerland). Extracted DNA was stored at –20 °C. The Primers Pmp1 (5′-CACCAGGTTGATTCTGCCTGAC-3′) and HG4r (5′-TGGTCCGTGTTTCAAGACGGG-3′) were selected to amplify the SSU, ITS and part of the LSU of the rDNA of *T. pectinatellae*, *B. plumatellae* and *P. cristatellae*, giving a product of about 2 kb (Zhu et al. 1993; Gatehouse and Malone 1998). Amplification was carried out in 50 µl volumes using the Expand Long Template PCR Kit (Roche, Rotkreuz, Switzerland). Part of the SSU rDNA of *B. tuftyi* was amplified with the primers MicU1 (5′-TGATTCTGCCTGACGTR GRYGC-3′) and MicU9r (5′-RRCATHKTTTACTGC WRGAACTA-3′) in order to check whether it was identical to *B. plumatellae*. These primers were designed to amplify a wide range of microsporidia and produce an amplicon of about 700 bp. As the product is shorter than that produced by Pmp1 and HG4r, the amplification is more robust and works better with difficult samples (Refardt et al. 2002). Amplification was carried out in 50 µl volumes using HotStarTaq DNA Polymerase (Qiagen, Basel, Switzerland). All amplicons were checked on a 1.5% agarose gel, excised and cloned in a Topo vector (Invitrogen, Groeningen, Netherlands). Purified plasmids were checked by digestion with EcoRI whether they contained the desired insert and analyzed by dye termination sequencing (Microsynth, Balgach, Switzerland).

Sequences of the 16S rDNA of 37 microsporidia and of *Basidiobolus ranarum* (Fungi: Zygomycetes) as the outgroup species were obtained from the GenBank. The microsporidian sequences were chosen to cover all prominent groups of the phylum and all lineages branching at the root of the phylum. These sequences and those from the new microsporidia from bryozoans (Table 1) were automatically aligned with Clustal X (Thompson et al. 1997) and edited visually using BioEdit 5.0.9 (Hall 1999). Primer sites at the 3′ and 5′ ends were truncated and characters that could not be aligned unambiguously as well as characters containing prominent gaps were removed leaving an alignment of 923 bp length. Analyses were carried out employing Bayesian inference (MRBayes 2.01) (Huelsenbeck and Ronquist 2002), maximum likelihood and parsimony (PAUP* 4.0b8) (Swofford 2000). To control for a possible influence of the truncated sequence of *B. tuftyi* on the general results of the phylogenetic analyses, all analyses were done with and without this sequence.

Bayesian inference

MRBayes was run using both the general reversible and the general non-reversible model. A proportion of sites was assumed to be invariable, while the rate of the remaining sites was drawn from a discrete gamma distribution with 8 categories. All parameters were inferred from the data. Four Markov chains were initiated at random and the program was allowed to run for 200,000 generations with sample frequency of 100. Likelihood convergence took 10,000 generations. These sampled trees were discarded as burn-in and the following trees were used to build a majority rule consensus tree with mean branch lengths.

Maximum likelihood

Maximum likelihood models were chosen by likelihood ratio tests and AIC criteria in Modeltest 3.06 (Posada and Crandall 1998). The selected models were TrN+I+G and GTR+I+G respectively. The search was done heuristically with random stepwise addition (10 replicates) and TBR branch swapping.

Parsimony

Constant and uninformative characters were removed prior to the analysis, leaving an alignment of 509 parsimony informative characters. Searches were done heuristically with random stepwise addition (10 replicates) and tree bisection and reconnection (TBR) branch swapping. A 90% majority rule consensus tree was generated by bootstrapping 100 times the original dataset. The consensus tree was imported into MacClade 3.01 (Maddison and Maddison 1997) together with the original dataset. Data were weighted using the rescaled consistency index and imported back into PAUP*. A majority rule consensus tree was generated by bootstrapping 500 times the weighted dataset using the 90% majority rule consensus tree as a constraint.

Results

Description of species

Trichonosema pectinatellae n.gen., n.sp.

The infected cells, which were freely circulating in the coelomic cavity of *P. magnifica* appeared rounded by light microscopy and measured 100–250 µm diameter. The infected cells had a simple plasma membrane raised as branched filopodial processes which were especially prominent at the surface of the smaller cells (Fig. 1). The host cells were multinucleate, with sections showing up to ten nuclear profiles with electron dense nucleolar material lining the nuclear envelope and dispersed in the centre (Fig. 3). The host cell cytoplasm contained cristate mitochondria, endoplasmic reticulum and multilamellar bodies (Fig. 5), the latter es-

pecially prominent in highly disorganised regions. Some profiles showed several stretches of muscle in otherwise disorganised cytoplasm (Figs 2, 4), providing clear evidence of the muscular nature of the infected tissue. In one cell, several profiles of a 9+2 microtubular structure were seen in transverse section, without the enveloping membrane of a cilium (Figs 7, 8). However numerous sections of cilia were observed in the coelomic fluid close to infected cells (Fig. 23). No parasites with more than one diplokaryon were seen, nor any stages undergoing cytoplasmic division but closely apposed pairs of cells at a similar stage of development suggested that cytoplasmic constriction occurred by binary fission in merogony and sporogony. All stages were in direct contact with host cell cytoplasm.

Meronts were highly irregular cells, sometimes with finger-like projections suggestive of amoeboid activity (Figs 6, 7). They had a simple plasmalemma, abundant rough endoplasmic reticulum and large diplokaryotic nuclei, occupying more than half the width of the meront, with uniformly granular nucleoplasm. Signs of nuclear division were limited to flat centriolar plaques (Fig. 9). In lightly-infected cells the outline of each meront was barely distinguishable from host cell cytoplasm (Fig. 6).

The onset of sporogony was signalled by the deposition at the surface of 30 nm electron-dense globules, patchily at first then as a regularly-spaced coat of globules (Fig. 10). Growth of the secretions gave rise first to separate pyramidal structures on the sporonts (Fig. 11), then to radiating, 90 nm high spikes on the sporoblasts (Fig. 14). The spikes were united at their base into a dense coat covering the plasmalemma (Fig. 15) and this coat with persistent, more hair-like spikes became the exospore layer of the spore wall (Fig. 20). Pairs of sporoblasts suggested that sporogony by binary fission occurred at the pyramidal stage of surface secretions (Figs 12, 13). Late sporoblasts, still lacking an endospore layer, showed a diplokaryon and a posteriorly-located convoluted Golgi apparatus in the form of a reticulum (Fig. 16).

Fresh spores were elongate pyriform (Fig. 24). The means and standard errors (n = 20) were 9.45 ± 0.3 µm × 4.45 ± 0.07 µm and the range was 8.0–11.0 µm × 4.0–5.25 µm. They did not fix well for electron microscopy but regions of different spores collectively provided details of the overall structure. The exospore was a 45 nm thick layer, thinned to 30 nm over the anchoring disc (Fig. 17). Spikes up to 220 nm high radiated from the whole surface. The endospore probably measured no more than 125 nm, thinned to 50 nm over the anchoring disc (Fig. 20) but appeared wider along the sides of many spores because of its separation from the sporoplasm. The anchoring disc was an ovoid structure with a dense boundary and a more lucent core penetrated by the funnel-like expansion of the anterior end of the polar tube (Fig. 17). The anchoring disc was enclosed in a rather small umbrella-like polar sac (Fig. 18). The two nuclei lay one behind the other, occupying the central region of the spore surrounded by rows of polyribosomes, while the posterior vacuole, full of amorphous material in the mature spore, occupied the posterior end (Fig. 20). The membranous component of the polaroplast was connected to the polar tube for only a short distance behind the anchoring disc (Fig. 20). From this region the tightly compacted membranes (Figs 19, 20) were directed posteriorly, sometimes curving inwards, and extended to about a quarter or one third of the cytoplasmic part of the spore, reaching the anterior level of the diplokaryon. Thus, the membranous polaroplast appeared in section as short lobes on both sides of the straight section of the polar tube. Internal to the lobed structure, around the polar tube, the organisation was less clear but mainly appeared as spherical vesicles. There were 25 or more coils of the polar tube around the nuclei and posterior vacuole (Fig. 21). Four or five of the most anterior coils were arranged in one layer, the middle coils in two or three layers and the last five or six coils in one layer. The structure of the coils in cross section is shown in Figure 22.

Bryonosema plumatellae n.gen., n.sp.

Infected cells as seen in living zooids were distinctly sausage-shaped measuring up to 500 µm and were free in the coelom of *P. nitens*. The surface of infected cells was covered by an abundance of branched, filopodial processes. The smaller cells of about 50 µm length were sometimes clustered, indicating that they had either become linked by the surface processes or, more likely, were just completing division, as cytoplasmic bridges were seen between them (Fig. 26). It is possible that the large, free-floating, sausage-shaped bodies were made up of several linked cells. The host cell nucleus, of which only one was seen per cell section, had an irregular outline and large and small accumula-

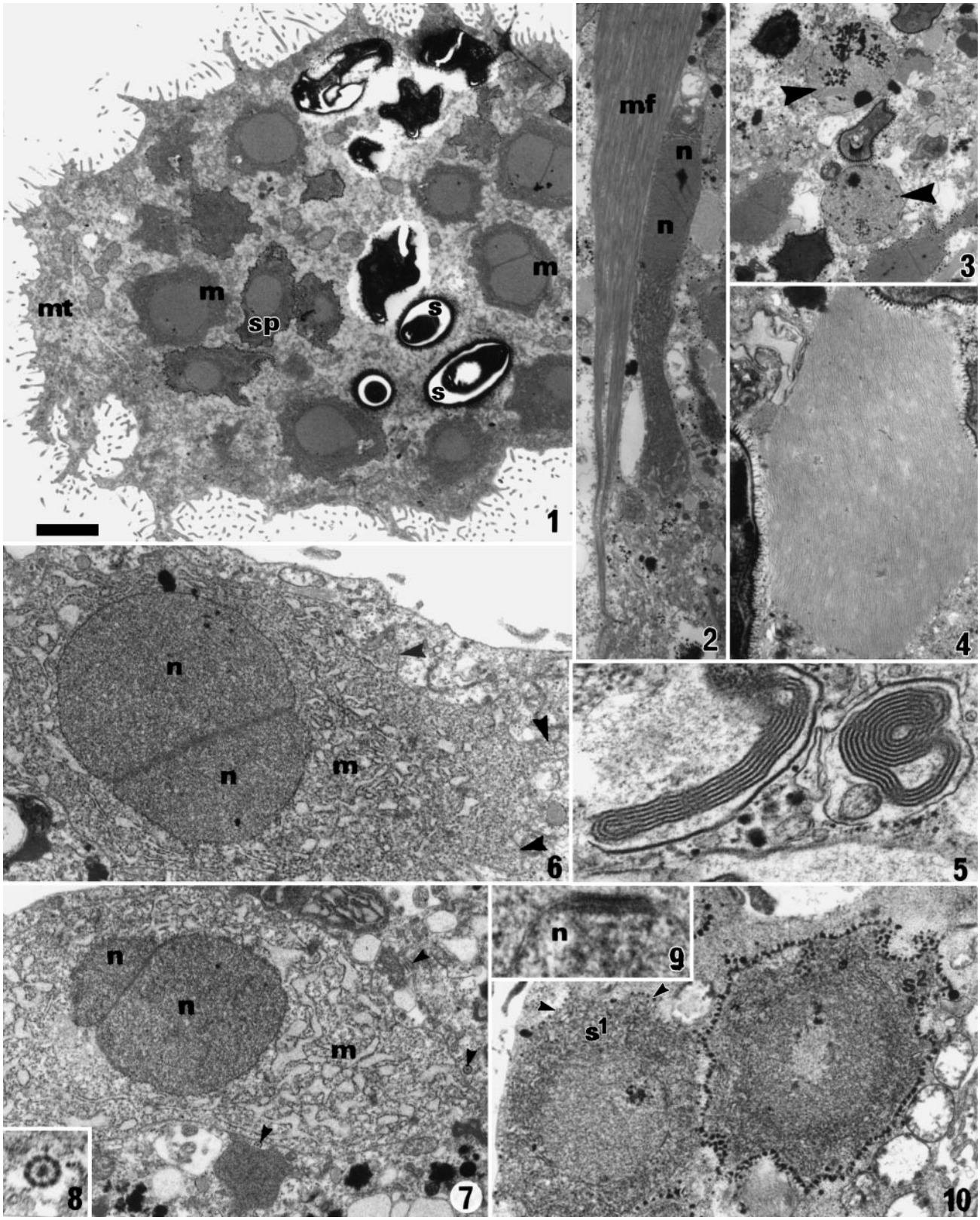
mt
m
sp
s
s
m
1
mf
n
n
2
3
4
n
n
m
6
5
n
n
m
8
7
n
9
s1
s2
10

tions of dense nucleolar fragments in a moderately dense, uniform nucleoplasm. The nucleus was located at the periphery of the cell where a degree of cytoplasmic integrity was maintained (Fig. 26). In the centre, the cytoplasm was reduced to a patchy granulation with lucent spaces, although apparently functional mitochondria with plate-like cristae were still present (Fig. 29).

Meronts were pale cells, of highly irregular outline, which showed moderate development of rough endoplasmic reticulum (Figs 27, 28). The diplokaryotic nuclei showed nucleolar fragments but in only one case was a centriolar plaque seen, as a sign of division.

At the onset of sporogony a dense rough exospore coat was deposited on the plasma-membrane. No stages were seen with separate patches of exospore. It was either present as a thin, uniform layer or was absent. Binary fission was indicated by the presence of mirror-image stages of sporoblasts, lying posterior to posterior (Fig. 29), while polar tube construction from the Golgi reticulum was evident. At this stage a dense sphere, 730 nm diameter, was present close to the Golgi reticulum. Maturation of sporoblasts to spores proceeded with the formation, from the posterior end, of additional coils of the polar tube to link up with the anchoring disc-polar sac complex laid down at the anterior end (Figs 30, 31). At this stage parallel cisternae of endoplasmic reticulum were visible around the diplokaryotic nuclei but the polaroplast had not been organised and the endospore layer was minimal.

Fresh spores were broadly pyriform and many showed a clear posterior vacuole (Fig. 25). Means and standard errors (n = 20) were 8.4 ± 0.4 µm × 5.8 ± 0.01 µm and the range was 7.5–10.0 µm × 5.0–6.25 µm. The exospore was a uniformly dense, 85 nm layer with a rough edge, thinned to 35 nm over the anchoring disc. The endospore was often distorted but probably measured no more than 250 nm and was as little as 85 nm in some mature spores. It was thinned to 35 nm over the anchoring disc. Internal structures were poorly preserved. The anchoring disc was ovoid with a dense border, open posteriorly at the point where it linked with the anterior end of the polar tube (Fig. 34). The polar sac enclosing the anchoring disc was tapered sharply and extended back for only a distance of 250 nm. Little detail could be discerned in the polaroplast. In section it appeared as wide lobes, probably composed of tightly-packed membranes as in *T. pectinatellae*, connecting with the polar tube near its anterior end for a distance of 1.7 µm behind the anchoring disc. The region between the unattached parts of the lobes and the polar tube appeared to be occupied by loosely-packed spheres. The lobes extended for no more than a third of the length of the spore. Up to 33 coils of the polar tube were observed, in most cases with the anterior 5 or 6 coils arranged in a single layer, the middle coils in two or three layers and the last five or six coils in a single layer (Fig. 32). The internal structure of the coils is shown in Fig. 33. At maturity the Golgi reticulum degenerated into a series of large and small homogeneous globules and the dense sphere was no longer visible as a separate entity.

Bryonosema tuftyi n.sp.

Infected cells, bearing a profusion of branched filopodial processes, were free in the coelom of *Plumatella* sp. (Fig. 35). The processes linked several cells together as in infections of *B. plumatellae*.

Figs 1–10. *Trichonosema pectinatellae* in *Pectinatella magnifica*. The 1.0 cm bar on 1 applies to Figs 1–10. **1.** Free-floating host cell in coelom packed with meronts (m), sporogonic stages (sp) and spores (s). Note filopodial extensions of host cell surface and mitochondria (mt). Bar = 2.7 µm. **2.** Band of muscle myofibres (mf) adjacent to an elongate meront with diplokaryotic nuclei (n). Bar = 3.0 µm. **3.** Host cell nuclei (arrowheads) in disrupted cytoplasm containing several microsporidia. Bar = 3.0 µm. **4.** Thick band of muscle in a host cell. Bar = 1.25 µm. **5.** Multilamellar bodies in disorganised cytoplasm of host cell. Bar = 280 nm. **6, 7.** Meronts (m) with diplokaryotic nuclei (n). Note irregular meront surfaces with finger-like projections (arrowheads in Fig. 6) into the host cell cytoplasm. Small arrowheads in Figure 7 point to 9+2 microtubular structures in TS and LS. Bar = 1.0 µm (Fig. 6) and 1.1 µm (Fig. 7). **8.** Enlargement of one of several 9+2 microtubular structures present in the host cell cytoplasm of Fig. 7. Bar = 300 nm. **9.** Centriolar plaque in the nuclear envelope of a meront (n = nucleus). Bar = 180 nm. **10.** Early sporont (s1) with sparse globules of exospore material (small arrowheads) and late sporont (s2) with exospore coat at the pyramidal stage. Bar = 1.0 µm.

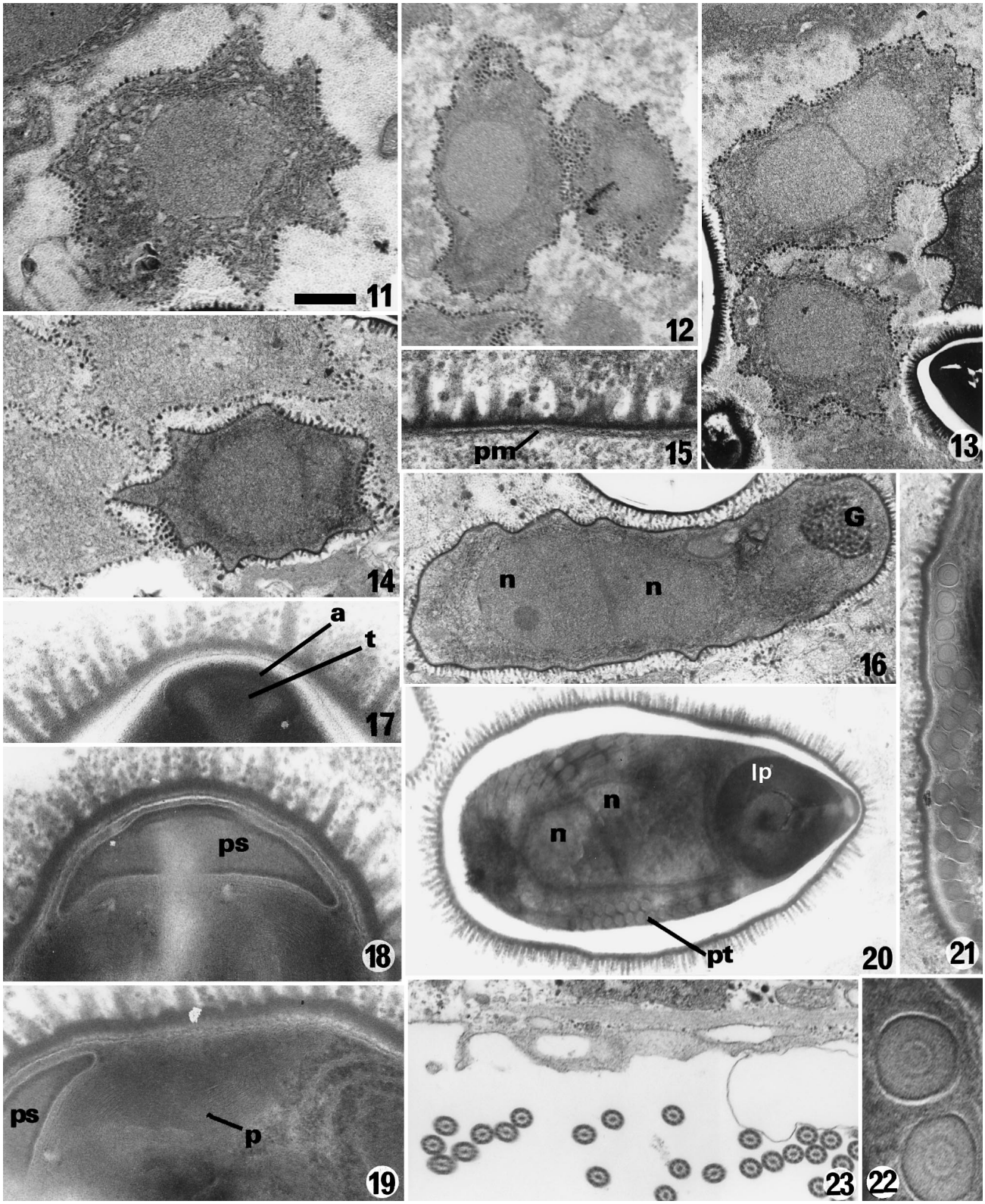
11
12
13
14
15
pm
16
G
n
n
17
a
t
18
ps
19
ps
p
20
lp
n
n
pt
21
22
23

The cytoplasm was packed with spores but only a few merogonic and sporogonic stages were present. The absence of myofibril clusters distinguished these cells from those infected with *T. pectinatellae*. Meronts were diplokaryotic cells with a simple plasma membrane and irregular outline (Fig. 36). The first sign of the transition to sporogony was the deposition of an amorphous layer of moderate density external to the plasma membrane (Fig. 37). This was followed by the gradual secretion of denser material from the plasma membrane outwards into the first layer producing a two-layered exospore, on the sporonts and sporoblasts (Figs 38, 40). Sporogonic stages were diplokaryotic but division was not seen. Polar filament formation was from a posteriorly-located Golgi apparatus but a Golgi-associated electron dense sphere, as in *P. plumatellae* was not apparent, although large homogeneous globules were seen in the Golgi area after synthesis of the polar tube (Fig. 39). Fresh spores were not available for measurement but dimensions of median sagittal sections in the resin blocks indicated a fresh size range of about 7.0–7.8 × 4.0–5.0 µm, after allowing for shrinkage of about 25%. Mature spores (Fig. 42) were more elongate than those of *B. plumatellae* and exhibited all the characters which typified the group of microsporidia from bryozoans i.e. ovoid anchoring disc in a small, tapered polar sac, membranous polaroplast forming lobes attached to the polar tube for a short distance and surrounding a vesicular region, polar tube coiled as a single layer anteriorly and posteriorly, and as two or three layers in the middle (Figs 42, 43). The exospore persisted as a double-layered structure on the mature spores (Fig. 41), although the external layer became almost invisible in prints which were light enough to reveal details of the internal structure (Fig. 42). Endospore measurements varied from 260 nm to 440 nm on different

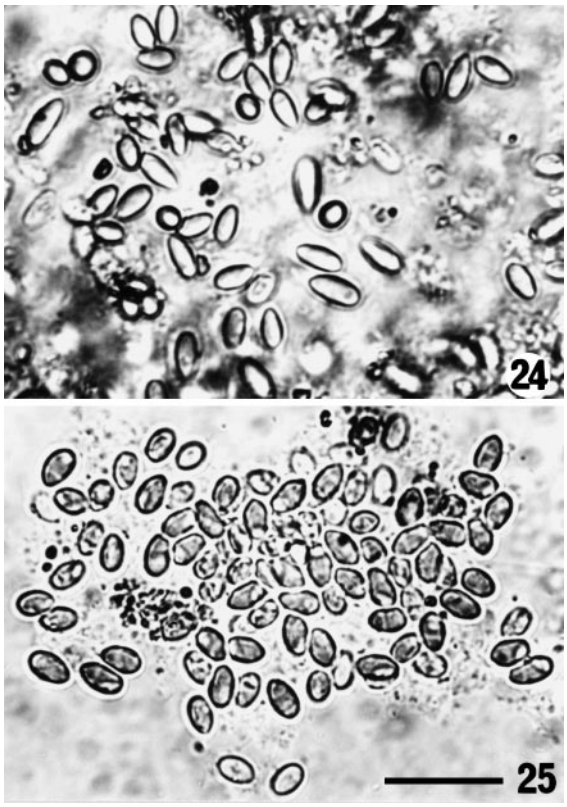

Figs 24–25. Fresh spores of *T. pectinatellae* (Fig. 24) and *Bryonosema plumatellae* (Fig. 25) released by pressure on host cells. Bar on Figure 25 = 20 µm and applies to both figures.

Figs 11–23. Sporogony of *Trichonosema pectinatellae*. The 1.0 cm bar on Figure 11 applies to Figures 11–23. **11.** Sporont with exospore at the pyramidal stage. Bar = 700 nm. **12, 13.** Division of sporonts with pyramidal exospore into two sporoblasts. Bar = 1.14 µm. **14.** Early sporoblast showing elongation of the pyramidal exospore structures and continuous basal layer of exospore. Bar = 1.0 µm. **15.** Surface of late sporoblast showing continuous exospore layer and its spiky extensions overlying the plasma membrane (pm). Bar = 170 nm. **16.** Late sporoblast with continuous exospore and spiky extensions showing nuclei (n) and Golgi reticulum (G). Bar = 830 µm. **17.** Anterior end of mature spore in median sagittal section showing spiky exospore coat, endospore and anchoring disc (a) penetrated by the inner tube (t) of the polar tube. Bar = 180 nm. **18.** Anterior end of immature spore lateral to the median sagittal section cutting through the polar sac (ps) but not the anchoring disc. Bar = 180 nm. **19.** Part of a longitudinal section of a spore on its side showing the polar sac (ps) and close-packed membranes of the polaroplast (p) running almost longitudinally. Bar = 180 nm. **20.** Mature spore showing spiky exospore and endospore, both thinned over the anchoring disc/polar sac complex, backwardly-directed lamellar polaroplast (lp), diplokaryotic nuclei (n) and coils of the polar tube (pt). Bar = 660 nm. **21.** Coils of the polar tube in an immature spore, showing arrangement in a single row anteriorly and posteriorly and in two or three rows in the middle. Bar = 400 nm. **22.** Polar tube coils in TS showing concentric layers. Bar = 100 nm. **23.** Sections of numerous cilia in the coelomic cavity close to a heavily infected cell. Bar = 590 nm.

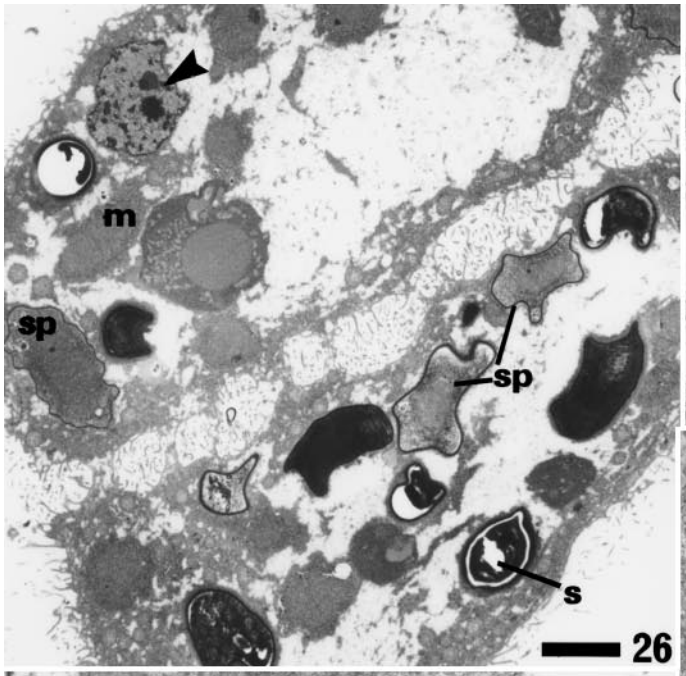
m
sp
sp
s
26

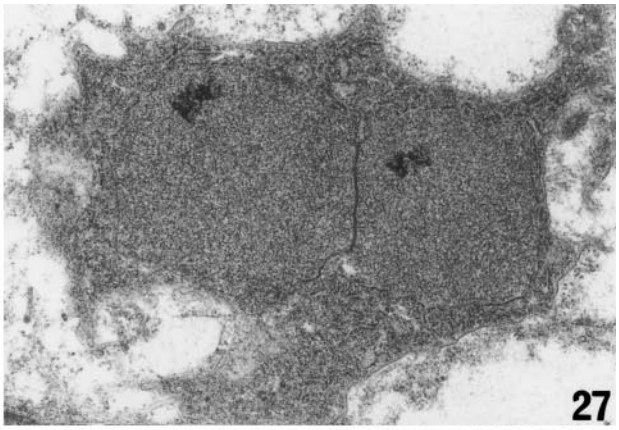
27

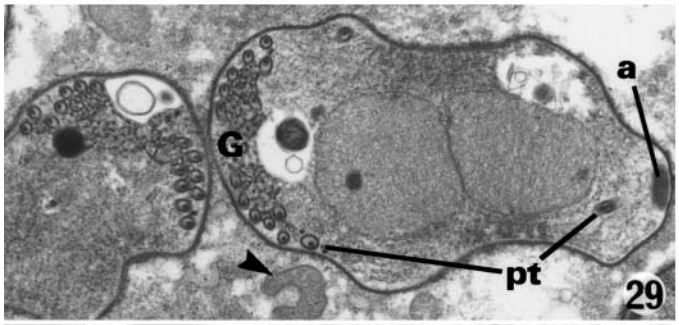
a
G
pt
29

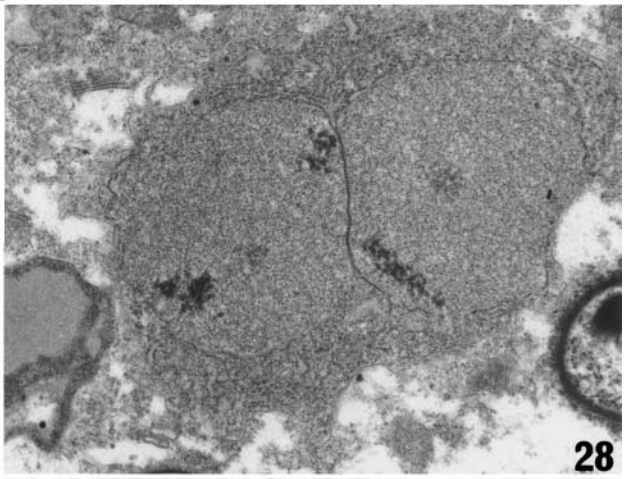
28

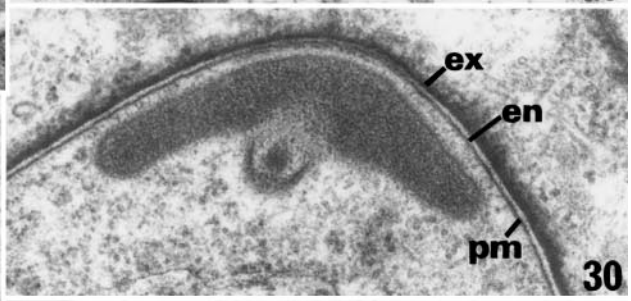
ex
en
pm
30

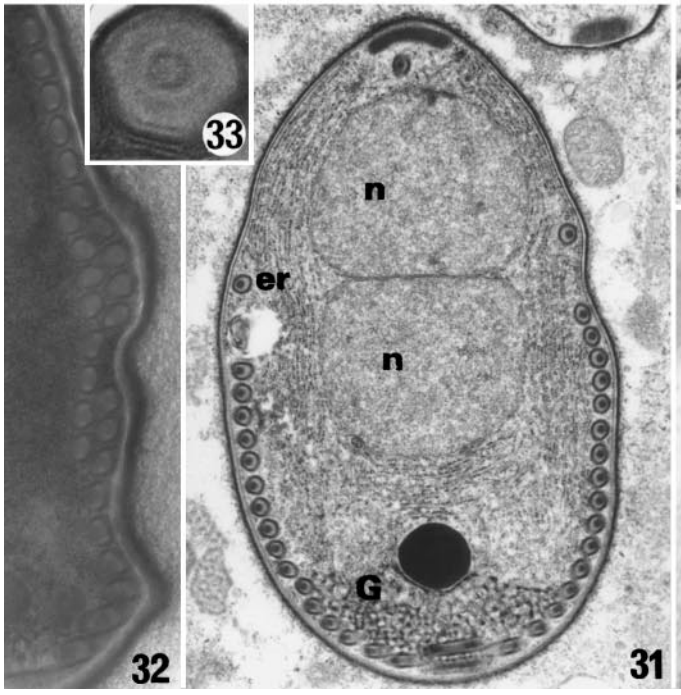
33
n
er
n
G
32
31

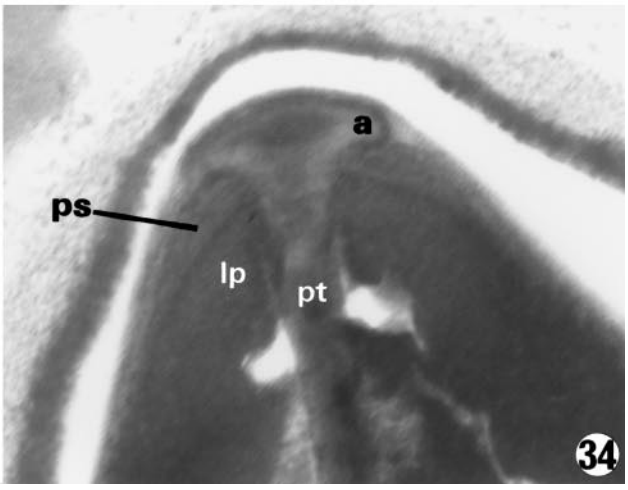
a
ps
lp
pt
34

spores and thinned to 50 nm over the anchoring disc. The inner layer of the exospore ranged from 130 nm to 180 nm and the outer layer from 140 nm to 103 nm on the corresponding spores.

Pseudonosema cristatellae n.gen.

New infections of *C. mucedo* confirmed previous observations (Canning et al. 1997) including infection restricted to hypertrophic cells in epithelial spaces.

Phylogenetic analysis of 16S rDNA sequences

Sequences of the SSU, ITS and part of the LSU of the rDNA were obtained for *T. pectinatellae*, *P. cristatellae* and *B. plumatellae*.

For *T. pectinatellae* one clone, which was sequenced in both directions, provided almost the full length sequence of the SSU rDNA. From another clone, a partial sequence was obtained which was 100% identical to the corresponding part of the full sequence. For the remaining species, sequences were obtained in one direction only.

A full SSU rDNA sequence was obtained for a clone of *P. cristatellae* as well as three partial sequences, which covered the beginning of the SSU. Comparable sequence fragments were >99% identical. For *B. plumatellae* 13 clones were studied from sample A of spores from Big Evans Lake, fixed in ethanol. Of these nine contained a sequence that was cut once when digested by EcoRI (clone 1) and four contained a sequence that was cut twice. Additionally, 11 clones were obtained from *B. plumatellae* DNA extracted from the spores in sample B from the same lake but retained in water. Among these clones, one was cut once by EcoRI and 10 were cut twice. Three different full sequences were obtained: clones 1 and 2 were from the ethanol fixed spores and clone 3 was from the fresh spore sample. Material from the same collection had been studied by em. Finally a partial sequence of 580 bp was obtained in the SSU of *B. tuftyi*. Sequences have been submitted to the GenBank under the accession numbers listed in Table 1.

The aligned 16S rDNA sequences of 37 microsporidia obtained from the data base together with the six sequences obtained from microsporidia in bryozoans and that of *Basidiobolus ranarum* as outgroup (Table 1), were analysed by Bayesian inference, maximum likelihood (ML) and parsimony. All methods revealed the same general tree topology with 8 clades (Fig. 44, A–H) that were supported by high confidence values (posterior probability = 100%, bootstrap values > 95%). An exception was clade H, where parsimony gave only 85% bootstrap support when *B. tuftyi* was included. The topologies of the trees found by Bayesian inference and ML were identical (Fig. 44), whereas parsimony differed by placing clade E at the root of clades A–D and *Flabelliforma magnivora*. None of the methods was able to resolve the relationship among the clades A–D/*F. magnivora*, G/H/*Antonospora. scoticae*, E and F unambiguously. However, the methods favoured a dichotomy that separated clades A–F/*F. magnivora* and G/H/*A. scoticae*.

Figs 26–34. *Bryonosema plumatellae* in *Plumatella nitens*. The 1.0 cm bar on Figure 26 applies to Figures 26–34. **26.** Free-floating host cells linked by filose extensions of their surfaces. Stages of merogony (m), sporogony (sp) and spores (s) are present in disorganised host cell cytoplasm. Arrowhead points to host cell nucleus. Bar = 3.0 µm. **27, 28.** Diplokaryotic meronts. Note that meronts are barely distinguishable from host cell cytoplasm. Bar = 830 nm (Fig. 27) and 770 nm (Fig. 28). **29.** Binary fission of a sporont into two sporoblasts. The well developed Golgi reticulum (G) is already producing the coils of the polar tube (pt), which has reached the anterior end close to the anchoring disc (a). Note the Golgi-associated dense spheres and intact host cell mitochondrion (arrowhead). Bar = 1.0 µm. **30.** Anterior end of immature spore in which a narrow endospore layer (en) is interposed between the exospore (ex) and plasma membrane (pm). The polar tube has made contact with the undifferentiated anchoring disc. Bar = 210 nm. **31.** Immature spore showing polar tube forming from the posteriorly-located Golgi reticulum (G), which has an associated dense sphere. Note layers of rough endoplasmic reticulum (er) around the diplokaryotic nuclei (n). The er cisternae extend towards the anchoring disc and may contribute to the polaroplast which is not yet evident. Bar = 770 nm. **32.** Polar tube coils in an immature spore arranged as a single row anteriorly and posteriorly and as two rows in the middle. Bar = 370 nm. **33.** Transverse section of a polar tube coil showing the concentric layers. Bar = 65 nm. **34.** Anterior end of mature spore showing junction of polar tube (pt) with the anchoring disc (a) and the sharply-pointed sections of the polar sac (ps) overlying the compact lamellae (lp) of the polaroplast. Bar = 150 nm.

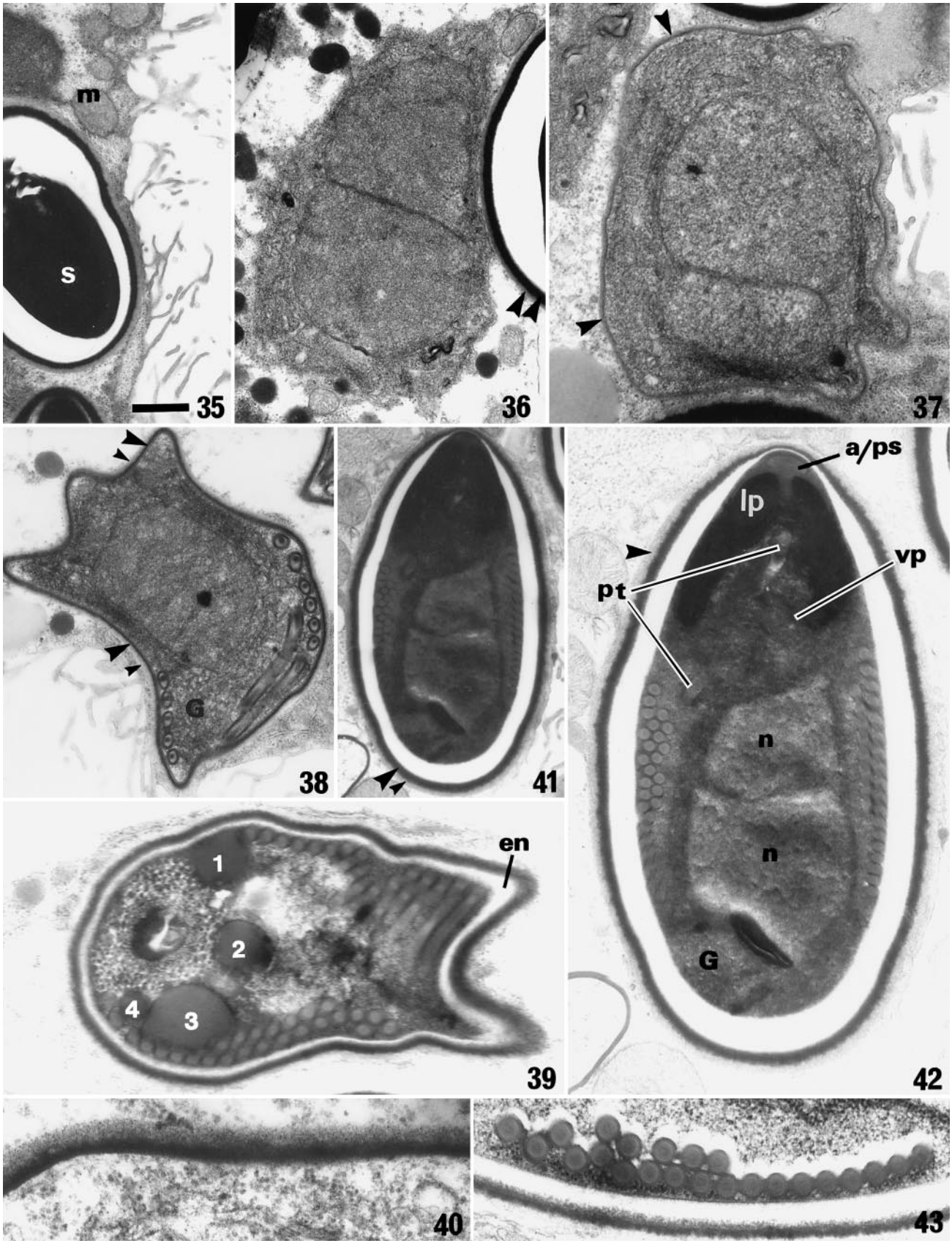
m
s
35
36
37
38
G
41
a/ps
lp
vp
pt
n
n
G
42
en
1
2
3
4
39
40
43

Table 2. Percent identity of pairwise comparison of microsporidian SSUrDNA based on the alignment used in the phylogenetic analysis. Number of nucleotide differences over the compared sequence length are given in brackets.

	B. plumatellae clone2	*B. plumatellae* clone3	*B. tuftyi*	*T. pectinatellae*	*P. cristatellae*	*J. debaisieuxi*	*Bacillidium* sp.	*N. bombycis*
B. plumatellae clone1	94 (82/1360)	86 (194/1389)	79 (122/580)	75 (343/1370)	76 (349/1456)	73 (377/1397)	73 (370/1372)	52 (667/1389)
B. plumatellae clone2		89 (153/1389)	79 (122/580)	78 (301/1369)	79 (306/1455)	76 (335/1396)	76 (329/1371)	53 (653/1389)
B. plumatellae clone3			75 (145/579)	78 (301/1367)	78 (320/1454)	75 (349/1394)	76 (328/1365)	54 (639/1367)
B. tuftyi								
T. pectinatellae					81 (268/1413)	77 (317/1378)	77 (317/1379)	54 (638/1386)
P. cristatellae						76 (347/1444)	77 (327/1421)	51 (710/1448)
J. debaisieuxi							87 (178/1366)	55 (628/1396)
Bacillidium sp.								54 (633/1376)

Figs 35–43. *Bryonosoma tuftyi* in *Plumatella* sp. The 1.0 cm bar on Figure 35 applies to Figures 35–43. **35.** External surface of a heavily infected host cell showing branched filose extensions. m = mitochondrion, s = spore. Bar = 1.0 µm. **36.** Diplokaryotic meront. Note the two layers of exospore (arrowheads) on the adjacent spore. Bar = 870 nm. **37.** Early sporont: note the layer of moderate density (arrowheads) on the plasma membrane. Bar = 625 nm. **38.** Sporoblast showing formation of the polar tube from the posterior end. Note the dense (arrowhead) and less dense layers (small arrowheads) of the exospore. Bar = 870 nm. **39.** Advanced sporoblast showing about 25 coils of the polar tube arising from the Golgi vesicles around which are four homogeneous globules (1, 2, 3, 4). The endospore layer (en) is forming. The less dense layer of exospore is barely visible in the light print. Bar = 480 nm. **40.** External surface of a sporoblast before the endospore is formed, showing the layers of differing density making up the exospore. Bar = 215 nm. **41.** Dark print of a mature spore, showing the two layers of exospore (arrowhead and small arrowhead). Bar = 1.01 µm. **42.** Enlargement and lighter print of the spore shown in Figure 41. The external layer of exospore is barely visible (arrowhead) but the internal structures are clear. Note the shape of the anchoring disc/polar sac complex (a/ps), lobes of the polaroplast (lp) joined only to the anterior quarter of the straight part of the polar tube (pt) and enclosing a vesicular polaroplast region (vp), diplokaryotic nuclei (n), coils of the polar tube arranged anteriorly and posteriorly as a single row and as two or three rows in the middle, and Golgi reticulum (G). The electron dense structure between the posterior nucleus and the Golgi reticulum may be an artifact. Bar = 510 nm. **43.** Arrangement of polar tube as single rows anteriorly and posteriorly and as two rows in the middle. Bar = 275 nm.

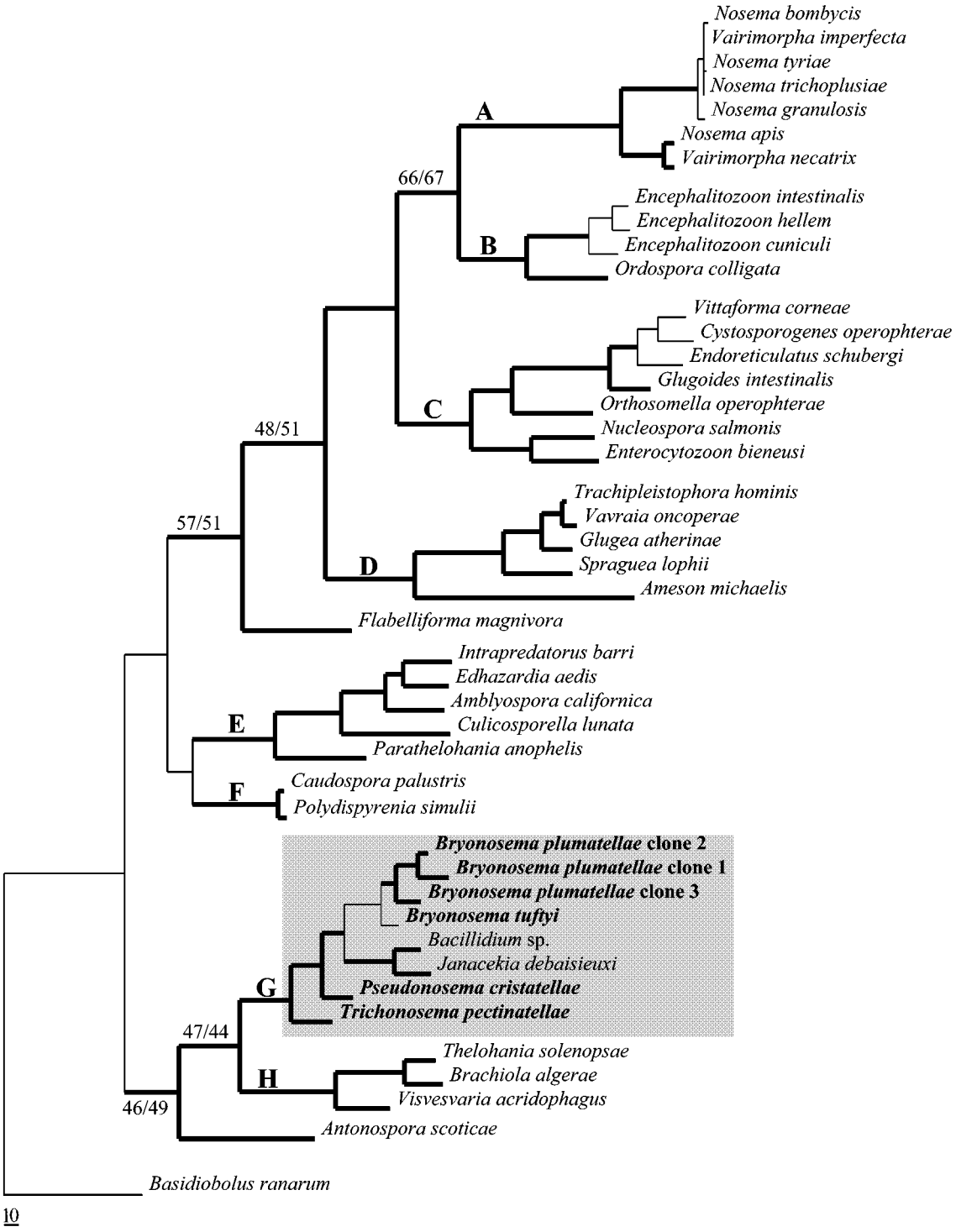

Fig. 44. Consensus tree obtained by Bayesian inference of 16S rDNA phylogeny. Topology as revealed by maximum likelihood is identical. Parsimony differs in placing clade E at the root of clades A–D and *F. magnivora*. Bold branches indicate posterior probabilities and bootstrap values ≥ 95%. Where parsimony gave no significant support in contrast to Bayesian inference, bootstrap values are given (with and without *Bryonosema tuftyi*).

Table 3. Pairwise identities between different sequences of *Bryonosema*. The sequences compared were adjusted to the length of the *Bryonosema tuftyi* fragment.

	B. plumatellae clone2	*B. plumatellae* clone3	*B.tuftyi*
B. plumatellae clone1	98 (564)	85 (566)	79 (588)
B. plumatellae clone2		85 (566)	79 (588)
B. plumatellae clone3			75 (587)

Microsporidia from all four bryozoan hosts fell into a single clade (G), which also encompassed *Bacillidium* sp. from an aquatic oligochaete, *Lumbriculus* sp., and *Janacekia debaisieuxi* from blackflies, *Simulium* sp. Basal to clade G was clade H with *Thelohania solenopsae*, *Brachiola algerae* (formerly *Nosema algerae*) and *Visvesvara acridophagus* (formerly *Nosema acridophagus*) and *A. scoticae*. The posterior probabilities of clades G/H and G/H/*A. scoticae* were ≥95% and 100% respectively. Bootstrap support as calculated by parsimony was between 40% and 50%. When *A. scoticae* was pruned from all bootstrapped trees, bootstrap values for clade G/H were raised to 81% (with *B. tuftyi*) and 83% (without *B. tuftyi*).

None of the microsporidia from bryozoans was close to the clade containing *N. bombycis*, the percent identity not exceeding 54%. The lengths of the sequences and the percent identities of the sequences of microsporidia in clade G and of *Nosema bombycis* are given in Table 2. The three *B. plumatellae* sequences gave identities of 94% (clone 1/clone 2), 86% (clone 1/clone 3) and 89% (clone 2/clone 3). Sequence difference between clones 1 and 2 was mainly due to a stretch of 138 bp in the 16S rDNA. This stretch contained several indels and point mutations and two thirds lay in a conserved region of 16S rDNA. When this region was excluded, identity was 98%. The ITS and the 482 bp of the 5′ end of the LSU were 100% identical in clones 1 and 2. Differences in clone 3 were not restricted to a small region of the SSU but were distributed in the SSU, ITS and LSU.

16S rDNA sequences obtained from *P. cristatellae* and *T. pectinatellae* had lengths of 1473 bp and 1423 bp. As we did not sequence the full length of the 16S rDNA of *T. pectinatellae*, total length is estimated. A partial sequence of *B. tuftyi* obtained from *Plumatella* sp. was 79%, 79% and 75% identical respectively with clones 1, 2 and 3 of *B. plumatellae* (Table 3). The sequences obtained for the *Bryonosema* spp. were more closely related to one another than to *P. cristatellae* and *T. pectinatellae* (Tables 2, 3).

In the absence of *B. tuftyi*, Bayesian inference and parsimony supported the topology in Fig. 44 by mostly high confidence values (≥ 95%). Parsimony gave only moderate support for the monophyly of *Bacillidium* sp., *Janacekia debaisieuxi* and *B. plumatellae* (66%) and the monophyly of those species together with *P. cristatellae* (67%). The inclusion of *B. tuftyi* destabilized parts of the topology: the monophyly of the *Bryonosema* spp. was supported by 84% (Bayesian inference) and 74% (parsimony). The monophyly of *Bacillidium* sp., *J. debaisieuxi* and *Bryonosema* spp. received 75% support by Bayesian inference, whereas parsimony supported this topology and a monophyly of *Bryonosema* spp. and *P. cristatellae* by equally low values (28 and 29%). Parsimony support for the monophyly of *Bacillidium* sp., *J. debaisieuxi*, *Bryonosema* spp. and *P. cristatellae* was low (57%).

Discussion

Ultrastructural data on all the microsporidia from bryozoans examined in this study, including *Nosema cristatellae* Canning, Okamura and Curry, 1997 demonstrate that they are remarkably similar in development and spore structure. The hallmarks of this group of microsporidia are large spores, generally exceeding 7.0 µm in length, characteristic ovoid anchoring disc within a small polar sac and a polaroplast of compact membranes, seen in section as backwardly directed lobes connected to the polar tube over a short, anterior distance and enclosing a region of small vesicles. There are upwards of 25 coils of the polar tube surrounding the diplokaryon, arranged as a single row anteriorly and posteriorly and as two or three rows in the middle.

There are few morphological characters which differentiate the four species from bryozoan hosts. *Trichonosema pectinatellae* is distinguished from

the other species by virtue of the exospore which is deposited patchily and has spiky extensions from a continuous basal layer on mature spores. The two *Bryonosema* spp. had exospores, which were deposited uniformly and lacked the spiky extensions. The species were distinguished by the number of exospore layers and the presence or absence of a Golgi-associated sphere. *P. cristatellae* differs from the other species in developing in hypertrophic host cells within defined spaces in the epithelium of *C. mucedo*, as opposed to free-floating cells in the coelom. Morphological similarity suggests that *P. cristatellae* would be placed in the same genus as the *Bryonosema* sp. were it not for the phylogenetic analysis (see below). The taxonomic value of exospore morphology in microsporidia has yet to be assessed. In *Ameson michaelis* and *Ameson pulvis*, microsporidia infecting the skeletal muscle of crustaceans, the exospore is covered by hair-like extensions similar to those in *T. pectinatellae*. However *Ameson nelsoni* another parasite of crustaceans was transferred into the genus *Perezia* by Vivarès and Sprague (1979) because the spores lacked the external 'hairs', although the life cycle and spore structure in other respects are notably similar. As *Perezia nelsoni* and *A. michaelis* are closely related on analysis of 16S rDNA sequence (see Discussion in Canning et al. 2002), it is possible that exospore characters are not reliable guides in microsporidian systematics.

All the species resemble the genus *Nosema* in being diplokaryotic, disporoblastic and developing in direct contact with host cell cytoplasm. Analysis of 16S rDNA sequences support the close relationships, suggested by morphology, of the species infecting bryozoans but do not uphold a relationship with the genus *Nosema*, the type species of which, *Nosema bombycis*, is a parasite of lepidopterans. Although all the species from bryozoans were resolved in a single clade (Fig. 44, clade G), the sequence identity was low and the species straddled the genera *Bacillidium* and *Janacekia* which, on morphological grounds would appear to be unrelated. There was strong support by Baysian analysis, and moderate support by parsimony, for this topology although we were not able to assess the phylogenetic position of *B. tuftyi* with confidence. Sequence variation in microsporidian 16s rDNA is usually accompanied by morphological and geographical differentiation (Moser et al. 2000) or differences of host species (Didier et al. 1995). *P. cristatellae* and the *Bryonosema* spp. are separated in the phylogeny, with *P. cristatellae* closer to *T. pectinatellae*. If the 16S rDNA analyses are at all meaningful, the *Bryonosema* sp. cannot belong to the same genus as *P. cristatellae* in spite of morphological similarity.

The three 16S rDNA sequences obtained for microsporidia in *P. nitens* differ by such a substantial margin that they would normally be considered as separate species. However two of the sequences (clones 1 and 2) were obtained from the same infection in one colony and nothing in the ultrastructural study of this material suggested that more than one species was present. The SSU sequences of clones 1 and 2 were closely related and their ITS regions were identical. This provides strong evidence that they belonged to the same species. The third sequence (clone 3) was obtained from a separate *P. nitens* colony collected from the same habitat, which was not investigated ultrastructurally. For lack of evidence we cannot assess the status of clone 3.

Natural infections may be initiated in a host from several infective stages giving a genetically mixed population, which may account for the sequence variation, especially of clade 3. Another explanation for the sequence variation is that different genes may be involved in stage specific expression, as is known for some malaria parasites with life cycles alternating between a vertebrate and mosquito (Li et al. 1997). A third explanation is that one or more may be pseudogenes. In a recent study of *Thelohania contejeani*, a microsporidium infecting crayfish muscle (*Astacus fluviatilis*), two copies of 1361 bp and 1311 bp of the 16S rDNA gene, differing by 7% were found in a 1:1 ratio (Lom et al. 2001). *T. contejeani* is a dimorphic parasite with two morphologically distinct sporogonies which are expressed simultaneously. The smaller 16S rDNA sequence was considered by the authors to be a pseudogene (Lom et al. 2001) and functional significance in the alternate sporogonies was not considered. Only one type of merogony and sporogony was apparent in *B. plumatellae* but dimorphism in alternate host(s) cannot be ruled out. The existence of a pseudogene has also been proposed for *Nosema bombycis* (Katayama et al. 2001). Primers, based on a putative pseudogene of the 16S rDNA from a silkworm (*Bombyx mori*) isolate of *N. bombycis*, only gave PCR amplicons when used with true *N. bombycis* and not with morphologically identical species from other hosts. Amplification of *N. bombycis* was obtained

with all isolates when general microsporidia primers were used. The reason for the sequence variation in *B. plumatellae* remains an open question.

The status of *B. tuftyi* from *Plumatella* sp. has also required consideration. The most obvious difference was in the exospore structure but the absence of the Golgi-associated sphere from *B. tuftyi* may also be significant. Over the partial sequence (579 bp) of the 16S rDNA *B. tuftyi* was more distant from the three clones of *B. plumatellae* than the clones were from each other (Table 3). The phylogenetic analysis places *B. tuftyi* closer to *B. plumatellae* than to the other microsporidia from bryozoans and we have named it as a new species in the genus *Bryonosema*.

Surprisingly, clade G, containing the microsporidia of bryozoans, also contains *Bacillidium* sp. from the annelid worm *Lumbriculus* sp. and *J. debaisieuxi* from blackflies *Simulium* sp. These genera separate *Bryonosema* from *Pseudonosema* and *Trichonosema* but their morphology does not suggest a close relationship. *Bacillidium* shares a diplokaryotic, disporoblastic life cycle with the new genera from bryozoans but the spores are distinctive in being rod-shaped, ten times longer than broad, with a long straight manubroid region of the polar tube and a short coil. The exospore produces a membrane-like external layer, which is released from the spore surface as a sac in the type species, *Bacillidium criodrili* (Larsson 1994a) but is not released in other species e.g. *Bacillidium strictum* (Larsson 1992). A membrane-like layer is not formed from the exospore in any of the species from bryozoans. In spite of the gross difference in shape, the spores of *Bacillidium* have in common with the species in bryozoans the attachment of the close-packed polaroplast membranes only to the anterior part of the polar tube and the formation of electron dense bodies near the Golgi reticulum, similar to those seen in *B. plumatellae*.

Janacekia debaisieuxi in blackflies is diplokaryotic only in merogony. The uninucleate spores, probably produced after meiosis in the sporont, are isolated individually in true sporophorous vesicles. As blackflies are haematophagous as adults, it is possible that these haploid spores are infective to an alternate host, as is probable for the genera in clade F and is known for several genera in clade E (Becnel 1994). It has been hypothesised that heterosporous, polymorphic life cycles involving several hosts are primitive and that simpler life cycles are derived by loss of one or other of the developmental sequences (Baker et al. 1997). The complete life cycles of the species in clade G are unknown and it is possible that *J. debaisieuxi* alone among them has retained a polymorphic cycle or that there are alternate hosts for the parasite of bryozoans.

Prominent Golgi-associated electron-dense spheres, as found in *B. plumatellae* are not common in microsporidia. The most prominent examples are illustrated but not described in *Microgemma hepaticus* by Ralphs and Matthews (1986), in *Tetramicra brevifilum*, where a possible role as a store of RNA was suggested (Matthews and Matthews 1980) and in *Trichoctosporea pygopellita*, where they were reportedly generated by the Golgi apparatus (Larsson 1994b). Their location in *B. plumatellae* close to the Golgi reticulum and their breakdown in mature spores, suggests that the material may contribute to formation of the polar tube as in *T. pygopellita*. It is notable that material of the same electron density is present in the Golgi reticulum and in the core and outer layer of the polar tube. Several electron dense spheres are present in spores of *B. criodrili* and these are also associated with the rather extensive Golgi system (Larsson 1994a).

The nature of the host cells infected with *T. pectinatellae* and *B. plumatellae* which were free-floating in the coelomic cavity, is enigmatic. No clues were provided by the host cells infected with *B. plumatellae* or *B. tuftyi*. However, the cells harbouring *T. pectinatellae* contained numerous patches and some quite long stretches of muscle suggesting that they were likely to have been myocytes, possibly liberated after infection of the retractor muscles of the lophophore or muscle cells of the funiculus. The presence of 9+2 microtubules in these host cells, in an arrangement typical of external cilia rather than the 9+0 basal bodies is curious but might be explained by the internalization of ciliary axonemes without membranes. Ciliated epithelial cells may absorb their axonemes on becoming free as coelomocytes, but the presence of myofibres in the cells infected with *T. pectinellae* makes it unlikely that the host cells were of epithelial origin. The host cells of *P. cristatellae* were identified as epithelial cells of the body wall at the bases of the lophophores and growing edge of the colony and were not free-floating in the coelomic cavity.

Taxonomic summary

The four microsporidia from freshwater bryozoans possess very uniform ultrastructural characters and belong to a single clade in a phylogenetic tree based on 16S rDNA analysis. We propose to establish a new family for them, which will have to exclude *Janacekia* and *Bacillidium* although these genera at present fall into the same clade. It is anticipated that inclusion of additional rDNA or other gene sequences from a greater number of microsporidian genera will improve the phylogeny and show that *Janacekia* and *Bacillidium* are not closely related to the species from bryozoans.

Pseudonosematidae fam. nov.

Diplokaryotic in all stages of development, which are in direct contact with host cell cytoplasm. Merogony by binary fission. Sporogony probably disporoblastic. Spores of known species are large (greater than 7.0 µm in length). Exospore granular, rough or with spiky extensions. Exospore and endospore thinner over anchoring disc. Anchoring disc ovoid with denser boundary and lucent interior penetrated by the inner core of the polar tube. Polar sac like a small umbrella, sharply tapered and pointed at its outer limit. Diplokaryon surrounded by numerous polar tube coils arranged as a single row anteriorly and posteriorly, and as two or three rows in the middle. Prominent Golgi reticulum, with or without an associated electron dense sphere in sporoblasts, becomes a posterior vacuole in mature spores.

Family name based on the generic name of the first described species.

Pseudonosema gen. nov. With characters of the family. Exospore granular, slightly rough, lacking spiky extensions and deposited as a uniform layer and remains thin. Golgi-associated electron-dense sphere absent. Generic name based on *Nosema* with the prefix *Pseudo*, implying 'false'.

Pseudonosema cristatellae (Canning, Okamura and Curry, 1997). Parasites in fixed cells of the epithelium of *Cristatella mucedo*. Spores 7.3 × 5.1 µm, broadly pyriform with prominent posterior vacuole. Exospore slightly rough and thin (40 nm). 16S rDNA: accession number AF484694.

Type species by monotypy. Synonym *Nosema cristatellae* Canning, Okamura and Curry, 1997. Type host: *Cristatella mucedo* Cuvier, 1798. Type locality: Beale Bird Park Lake, Berkshire, U.K. Specific name based on the host's generic name.

Trichonosema gen. nov. With characters of the family. Exospore deposited as separate globules, which become pyramidal before forming a spiky coat united by a continuous basal layer. Golgi-associated electron dense sphere absent. Generic name based on *Nosema* with the prefix *Tricho* meaning 'hair'.

Trichonosema pectinatellae sp. nov. With characters of the genus. Parasites of cells derived from muscle, detached and free-floating in coelom of *Pectinatella magnifica*. Spores 9.5 × 4.5 µm elongate pyriform. 16S rDNA: accession number AF484695.

Type species by monotypy. Type locality: Cowan Lake, Ohio, U.S.A. Type host: *Pectinatella magnifica* (Leidy, 1851). Specific name based on the host's generic name.

Bryonosema gen. nov. With characters of the family. Exospore rough, composed of one thick layer or two layers of different density, without spiky extensions. Golgi-associated electron dense sphere present or absent. Generic name based on *Nosema* with the prefix *Bryo*, indicating the host's phylum.

Bryonosema plumatellae sp. nov. With characters of the genus. Parasites of cells of unknown origin, free floating in coelom of *Plumatella nitens*. Spores 8.4 × 5.8 µm broadly pyriform. Exospore rough, composed of one layer. Golgi-associated electron dense sphere present. 16S rDNA: three different sequences obtained, accession numbers AF484690, AF484691 and AF484692.

Type species by monotypy. Type host: *Plumatella nitens* Wood, 1996. Type locality: Big Evans Lake, Michigan, U.S.A. Specific name based on the host's generic name.

Bryonosema tuftyi sp. nov. Parasites of cells of unknown origin, detached and free-floating in coelom of *Plumatella* sp. Spores 7.0–7.8 × 4.0–5.0 µm (estimated from resin blocks) elongate pyriform. Golgi-associated electron dense sphere not observed. Exospore composed of two layers of different density. 16S rDNA: partial sequence, accession number AF484693. Type species by monotypy. Type host: *Plumatella* sp.

Type locality: Tufty's Corner Lake, Berkshire, U.K. Specific name based on the type locality.

Acknowledgements: We are grateful to Trish Rowland for assistance with electron microscopy and to the Natural Environmental Research Council for financial assistance (Grant No. GR9/04271).

References

Baker M. D., Vossbrinck C. R., Becnel J. J. and Maddox J. V. (1997): Phytogenetical position of *Amblyospora* Hazard and Oldacre (Microspora: Amblyosporidae) based on small subunit rRNA data and its implication for the evolution of the microsporidia. J. Eukaryot. Microbiol. 44, 220–225.

Becnel J. J. (1994): Life cycles and host-parasite relationships of microsporidia in culicine mosquitoes. Fol. Parasitol. 41, 91–96.

Canning E. U., Curry A. and Overstreet R. M. (2002): Ultrastructure of *Tuzetia weidneri* sp.n. (Microsporidia: Tuzetiidae) in skeletal muscle of *Litopenaeus setiferus* and *Farfantepenaeus aztecus* (Crustacea: Decapoda) and new data on *Perezia nelsoni* (Microsporidia: Pereziidae) in *L. setiferus*. Acta Protozool. 41, 63–77.

Canning E. U., Okamura B. and Curry A. (1997): A new microsporidium *Nosema cristatellae* n.sp. in the bryozoan *Cristatella mucedo* (Bryozoa, Phylactolaemata). J. Invertebr. Pathol. 70, 177–183.

Didier E. S., Vossbrinck C. R., Baker M. D., Rogers B. L., Bertucci D. C. and Shadduck J. A. (1995): Identification and characterization of three *Encephalitozoon* strains. Parasitology 111, 411–422.

Gatehouse H. S. and Malone L. A. (1998): The ribosomal RNA gene of *Nosema apis* (Microspora): DNA sequence for small and large subunit rRNA genes and evidence for a large tandem repeat size. J. Invertebr. Pathol. 71, 97–105.

Hall T. A. (1999): BioEdit: a user-friendly biological sequence alignment editor and analysis program for Windows 95/98/NT. Nucleic Acids Symposium Series 41, 95–98.

Huelsenbeck J. P. and Ronquist F. R. (2002): MRBAYES: Bayesian inference of phylogeny. Bioinformatics 17, 754–755.

Katayama Y., Iwano H., Hatakeyama Y., Inoue T., Canning E. U. and Ishihara R. (2001): Use of PCR with the specific primers for discrimination of *Nosema bombycis*. J. Sericult. Sci. Japan 70, 43–48.

Korotneff A. (1892): *Myxosporidium bryozoides*. Z. Wissenschaft. Zool. 53, 591–596.

Labbé A. (1899): Sporozoa. In: Butschli O. (ed.): Das Tierreich, Part 5, p. 180. Friedlander, Berlin.

Larsson J. I. R. (1992): The ultrastructural cytology of *Bacillidum strictum* (Léger and Hesse, 1916) Jirovec, 1936 (Microspora, Bacillidiidae). Europ. J. Protistol. 28, 175–183.

Larsson J. I. R. (1994a): Characteristics of the genus *Bacillidum* Janda, 1928 (Microspora, Mrazekiidae) – reinvestigation of the type species *B. criodrili* and improved diagnosis of the genus. Europ. J. Protistol. 30, 85–96.

Larsson J. I. R. (1994b): *Trichoctosporea pygopellita* gen. et sp. nov. (Microspora, Thelohaniidae), a microsporidian parasite of the mosquito *Aedes vexans* (Diptera, Culicidae). Arch. Protistenkd. 144, 147–161.

Li J., Gutell R. R., Danberger S. H., Wirtz R. A., Kissinger J. C., Rogers M. J., Sattabongkot J. and McCutchan T. F. (1997): Regulation and trafficking of three distinct 18S ribosomal RNAs during development of the malaria parasite. J. Mol. Biol. 269, 203–213.

Lom J., Nilsen F. and Dyková I. (2001): *Thelohania contejeani* Henneguy, 1892: dimorphic life cycle and taxonomic affinities, as indicated by ultrastructural and molecular study. Parasitol. Res. 87, 860–872.

Maddison W. P. and Maddison D. R. (1997): MacClade: analysis of phylogeny and character evolution. Sinauer Associates, Sunderland, Massachusetts.

Matthews R. A. and Matthews B. F. (1980): Cell and tissue reactions of turbot *Scophthalmus maximus* (L.) to *Tetramicra brevifilum* gen.n., sp.n. (Microspora). J. Fish Dis. 3, 495–515.

Moser B. A., Becnel J. J. and Williams D. F. (2000): Morphological and molecular characterization of the *Thelohania solenopsae* complex (Microsporidia: Thelohaniidae). J. Invert. Pathol. 75, 174–177.

Posada D. and Crandall K. A. (1998): MODELTEST: testing the model of DNA substitution. Bioinformatics 14, 817–818.

Ralphs J. R. and Matthews R. A. (1986): Hepatic microsporidiosis of juvenile grey mullet *Chelon labrosus* (Risso), due to *Microgemma hepaticus* gen. nov. sp. nov. J. Fish Dis. 9, 225–242.

Refardt D., Canning E. U., Mathis A., Cheney S. A., Lafranchi-Tristem N. J. and Ebert D. (2002): Small subunit ribosomal DNA phylogeny of microsporidia that infect *Daphnia* (Crustacea: Cladocera). Parasitology 124, 381–389.

Swofford D. L. (2000): PAUP*. Phylogenetic Analysis Using Parsimony (*and other methods). Sinauer Associates, Sunderland, Massachusetts.

Thélohan P. (1895): Recherches sur les Myxosporidies. Bull. Sci. France et Belge. 26, 100–394.

Thompson J. D., Gibson T. J., Plewniak F., Jeanmougin F. and Higgins D. G. (1997): The CLUSTAL_X windows interface: flexible strategies for multiple sequence alignment aided by quality analysis tools. Nucleic Acids Res. 25, 4876–4882.

Vivarès C. P. and Sprague V. (1979): The fine structure of *Ameson pulvis* (Microspora, Microsporida) and its implications regarding classification and chromosome cycle. J. Invertebr. Pathol. 33, 40–52.

Zhu X., Wittner M., Tanowitz H. B., Cali A. and Weiss L. M. (1993): Nucleotide sequence of the small ribosomal RNA of *Encephalitozoon cuniculi*. Nucleic Acids Res. 21, 1315.